This is a preprint version of the article published in:
Journal of the Acoustical Society of America, Vol. 137, No. 6, pp. 3232-3243 (2015).
http://dx.doi.org/10.1121/1.4919806

Please, cite this document as:
T. G. ZIELIŃSKI. "Normalized inverse characterization of sound absorbing rigid porous media." *Journal of the Acoustical Society of America*, Vol. **137**, No. 6, pp. 3232-3243 (2015).
DOI: 10.1121/1.4919806

Normalized inverse characterization of sound absorbing rigid porous media

TOMASZ G. ZIELIŃSKI
Institute of Fundamental Technological Research, Polish Academy of Sciences
ul. Pawinskiego 5B, 02-106 Warsaw, Poland
e-mail: tzielins@ippt.pan.pl

Abstract

This paper presents a methodology for the inverse characterization of sound absorbing rigid porous media, based on standard measurements of the surface acoustic impedance of a porous sample. The model parameters need to be normalized to have a robust identification procedure which fits the model-predicted impedance curves with the measured ones. Such a normalization provides a substitute set of dimensionless (normalized) parameters unambiguously related to the original model parameters. Moreover, two scaling frequencies are introduced, however, they are not additional parameters and for different yet reasonable assumptions of their values the identification procedure should eventually lead to the same solution. The proposed identification technique uses measured and computed impedance curves for a porous sample not only in the standard configuration, that is, set to the rigid termination piston in an impedance tube, but also with air gaps of known thicknesses between the sample and the piston. Therefore, all necessary analytical formulas for sound propagation in double-layered media are provided. The methodology is illustrated by one numerical test and by two examples based on the experimental measurements of the acoustic impedance and absorption of porous ceramic samples of different thicknesses and a sample of polyurethane foam.

Key words: inverse identification, porous media, acoustic impedance, sound absorption.

I. INTRODUCTION

The energy of acoustic waves penetrating into porous media filled with air (or other fluid) is usually very well dissipated by the viscous and thermal interactions of the pore-fluid with the solid frame/skeleton. For many materials with open porosity and a sufficiently rigid frame, only the propagation in the pore-fluid need to be considered to model this phenomenon. A typical approach is then to substitute such a rigid porous medium by an equivalent dispersive fluid characterized by the complex and frequency-dependent effective bulk modulus and density. There are in fact many models of that sort which have been proposed for various materials. The simplest of them are purely empirical and involve only a couple of parameters, such as, for example, the flow resistivity, in the models of Dealny and Bazley[1] with important generalizations proposed by Miki[2,3], which are valid for fibrous absorbent materials of very high porosity (originally they were proposed and validated for fibrous materials with porosity close to unity). More complicated models are less restrictive, yet they involve more parameters related to the average pore geometry. Thus, for example, Attenborough[4] proposed a model for rigid fibrous absorbents and granular materials using five parameters: porosity, flow resistivity, tortuosity, a steady flow shape factor, and a dynamic shape factor. More recently, new empirical models for fibrous materials have been proposed by Voronina[5], and for granular media by Voronina and Horoshenkov[6].

A general semi-phenomenological model for sound absorbing porous media with rigid frames was originally formulated by Johnson *et al.*[7] and substantially extended later by Champoux and Allard[8], and by Lafarge *et al.*[9] to include thermal losses in the porous medium. Other important improvements were introduced by Pride *et al.*[10]. It is a versatile model, based on a set of independently measurable porous material parameters. It is essentially formulated in the frequency domain, although recently time-domain formulations have been proposed (see, for example, a time-domain formulation without any restrictions on the frequency bands by Umnova and Turo[11]). In its standard version[12], which may be referred to as the Johnson–Champoux–Allard–Lafarge model (JCAL)[13], it uses six parameters: the total open porosity, the high frequency limit of the tortuosity (i.e., the classic parameter of tortuosity), the static viscous permeability (originally, the static air flow resistivity), the static thermal permeability, and two characteristic lengths—a viscous one and a thermal one. A slightly simplified version does not use the thermal permeability parameter and is usually called the Johnson–Champoux–Allard model (JCA). One the other hand, the enhanced eight-parameter version, which may be referred to as the Johnson–Champoux–Allard–Pride–Lafarge model (JCAPL)[13], also involves the static viscous and thermal tortuosities, which are in fact the low-frequency limits of their dynamic counterparts. As in most of the other models of porous media, there are also additional parameters representing some of the properties of the fluid in the pores, which are usually well-known. The JCA, JCAL or JCAPL model is often simply called the Johnson–Allard model. Its importance is also confirmed by the fact that, together with all parameters, the Johnson–Allard formulas are present in the Biot–Allard model for poroelastic media[12], which is essentially based on Biot's equations of poroelasticity instead of the Helmholtz equation for time-harmonic acoustics. The poroelastic model for sound absorbing media must be used when the vibrations of the solid frame cannot be neglected, for example, in the case of soft porous media or in active systems involving porous materials[14–16].

The essential parameters of the Johnson–Allard (JCA, JCAL or JCAPL) and Biot–Allard models which result from the microgeometry of the solid frame are in fact some sort of macroscopic, average geometric characteristics of the porous medium derived on the basis of homogenization theory. Although, they can be measured directly (see, for example, Refs.[17–20]), a specific measurement equipment is required for each one of them. This is an important reason for developing inverse methods of parametric identification based on acoustical measurements carried out by a single type of equipment.

The inverse characterization of porous media based on acoustical measurements has been investigated for various models and parameters. Braccesi and Bracciali[21] applied a least squares regression based on measured reflection coefficient values of sound absorbing porous specimens to estimate reliable values for the flow resistivity and structure factors used as parameters by an early model proposed by Zwikker and Kosten[22]. Alba *et al.*[23] applied an inverse identification method to obtain the porosity, fibre diameter, and density of fibrous sound absorbing materials using the Voronina model[5,24]. Fellah *et al.*[25] used reflected and transmitted ultrasonic waves in air-saturated industrial plastic foams in order to identify their porosity, tortuosity, and characteristic lengths. They applied the least squares method to solve numerically the inverse problem defined in the time domain. Göransson *et al.*[26] proposed a methodology for the inverse estimation of the anisotropic flow resistivity through porous materials. This methodology was then refined by Van der Kelen and Göransson[27], who applied it to identify the full anisotropic flow resistivity tensor of multiple glass wool and melamine foam samples.

An inverse identification of some parameters governing viscous dissipation in porous media was essayed by Panneton and Olny[28], who showed that when the open porosity and static airflow resistivity are known from direct measurements, and the dynamic density is obtained from acoustical techniques involving an impedance tube, the analytical solutions derived from the Johnson *et al.*[7] model yield the geometrical tortuosity and viscous characteristic length. The same authors[29] proposed a method for the inverse acoustical determination of the parameters governing thermal dissipation in porous media. Their approach is based on the measurement of the dynamic bulk modulus of the material (using a three-microphone method), and the analytical inverse solutions derived from three different semi-phenomenological models governing the thermal dissipation of the acoustic waves in porous media. In all three cases, the knowledge (i.e., a direct measurement) of the open porosity was assumed, and the inverse method was used to determine one or two of the remaining model parameters: for example, the thermal characteristic length and thermal permeability.

An ultrasonic characterization of homogeneous rigid porous materials based on the JCA model was proposed by Groby *et al.*[30]. The same model was used in inverse characterization by Dauchez and Yvars[31]. A good review on the inversion problems for determining parameters of porous materials has been recently published by Bonfiglio *et al.*[32]. Acoustical measurements in an impedance or standing wave tube were used to identify the parameters of the JCAL model by Sellen *et al.*[33], and also by Atalla and Panneton[34] for the JCA model. In that latter paper, the inverse characterization is applied only for three parameters, namely, the tortuosity and two characteristic lengths, which means that the open porosity, airflow resistivity, and bulk modulus must be measured with

direct methods. In that paper, only the standard configuration of a porous sample set directly to the rigid termination in the tube was used. Moreover, no direct parameter normalization was applied. Such a normalization, suitable for the inverse identification of the JCAL model parameters, has been recently proposed by Zielinski[35] in an approach which assumes that the open porosity is known. The present paper is an extension and continuation of conference reports by Zielinski[35,36], and it provides complete discussions as well as some new results. Here, the proposed methodology involves measuring of the surface acoustic impedance of porous samples in an impedance tube with air gaps (of known thicknesses) between the sample and the rigid termination of tube. This paper is organized as follows. First, the necessary formulas of the JCAL and JCAPL models are recalled. Then, the analytical solutions for plane harmonic wave propagation in double- and single-layered media are derived, together with formulas for the surface acoustic impedance and absorption coefficient. These formulas are used by the inverse identification procedure, applying the least squares method to a set of normalized dimensionless parameters proposed for the JCAL and JCAPL models. The procedure is illustrated by one test based on a numerical experiment (with synthetic data implying non-trivial identification[37]) and by the validated parametric identification of an open-porosity alumina foam based on measurements of two samples (of different thicknesses) carried out in an impedance tube, and finally, by another test based on the impedance-tube measurements of a polyurethane foam.

II. MODELING THE ACOUSTIC IMPEDANCE AND ABSORPTION OF POROUS MATERIALS

A. Sound propagation in porous media with a rigid frame

When the skeleton of a porous material can be regarded as rigid and motionless, which is common in materials like ceramic or metal foams and even for many softer (PU) foams, the time-harmonic acoustic wave propagation in such media can be effectively modeled as in fluids by using the classical Helmholtz equation of linear acoustics. In fact, a layer of the rigid porous material is then substituted by an effective fluid layer characterized by the *effective* speed of sound c and density ϱ, which should differ from the speed of sound of the fluid in the pores (typically, air), even for materials of very high porosity (which is usually the case for soundproofing materials). In consequence, the *effective* bulk modulus K is also introduced since $c^2 = K/\varrho$. Moreover, it is observed that porous materials are dispersive, therefore, the effective quantities should be frequency-dependent functions, namely, $c = c(\omega)$, $\varrho = \varrho(\omega)$, and $K = K(\omega)$ (here and below, $\omega = 2\pi f$ is the angular frequency, f is the frequency).

The effective density of a porous material is related to the density ϱ_f of the actual fluid filling the pores:

$$\varrho(\omega) = \frac{\varrho_\mathrm{f}\,\alpha(\omega)}{\phi}, \tag{1}$$

where ϕ is the open porosity and α is a dimensionless function of frequency, the so-called dynamic (visco-inertial) tortuosity. Johnson *et al.*[7] proposed a model for the dynamic tortuosity, which (apart from the kinematic viscosity, ν_f, of the fluid in the pores) depends on four geometric parameters that macroscopically characterize a porous medium, namely: the open porosity, ϕ, the (static) permeability, k_0, the tortuosity of the pores, α_∞, and finally, the characteristic size of the pores for the viscous forces, Λ. The static permeability is an intrinsic property of a porous medium, used, for example, in Darcy's law, where it relates the pressure gradient and the flux, which, when divided by the total porosity, is equal to the (average, macroscopic) velocity of stationary-flow (therefore, at $\omega = 0$). The tortuosity α_∞ is defined as the ratio of the hypothetical effective density of a porous medium saturated by an ideal, inviscid fluid, to the density of this fluid. Therefore, it takes into account only the inertial resistance, and in reality, when the saturating fluid is viscous, the effective density must only approach the value $\alpha_\infty\varrho_\mathrm{f}/\phi$ when the viscous skin depth tends to zero and the viscosity effects become negligible, that is, when $\omega \to \infty$. Johnson's model was modified by Pride *et al.*[10], and the improved version can be presented as follows:

$$\alpha(\omega) = \alpha_\infty + \frac{\nu_\mathrm{f}}{\mathrm{i}\omega}\frac{\phi}{k_0}\left[\sqrt{\frac{\mathrm{i}\omega}{\nu_\mathrm{f}}\left(\frac{2\alpha_\infty k_0}{\Lambda\phi}\right)^2 + b^2} - b + 1\right], \tag{2}$$

where b is a parameter introduced by Pride to adjust the low-frequency limit of the real part of the effective density (for circular pores, this limit is obtained at $b = 3/4$). Lafarge showed that the right low-frequency limit α_0 for the real part of α (i.e., $\lim_{\omega\to 0}\mathrm{Re}\,\alpha = \alpha_0$) is achieved when

$$b = \frac{2\alpha_\infty^2 k_0}{\Lambda^2\phi(\alpha_0 - \alpha_\infty)}. \tag{3}$$

An analysis of thermal effects leads to the following expression for the effective bulk modulus

$$K(\omega) = \frac{K_\mathrm{f}}{\phi\beta(\omega)}, \qquad \beta(\omega) = \gamma_\mathrm{f} - \frac{\gamma_\mathrm{f} - 1}{\alpha'(\omega)} \tag{4}$$

where $K_\mathrm{f} = \gamma_\mathrm{f}P_\mathrm{f}$ is the bulk modulus of the pore-fluid (P_f is the ambient mean pressure), γ_f is the heat capacity ratio for the pore-fluid, and α' is the frequency-dependent thermal tortuosity. This function was introduced by Lafarge[9] as an an analogue of the dynamic tortusity. Similarly, the following model was proposed for this quantity:

$$\alpha'(\omega) = 1 + \frac{\nu'_\mathrm{f}}{\mathrm{i}\omega}\frac{\phi}{k'_0}\left[\sqrt{\frac{\mathrm{i}\omega}{\nu'_\mathrm{f}}\left(\frac{2k'_0}{\Lambda'\phi}\right)^2 + b'^2} - b' + 1\right]. \tag{5}$$

where $\nu'_\mathrm{f} = \nu_\mathrm{f}/N_\mathrm{f}$, with N_f being the Prandtl number of the pore-fluid, while k'_0 is the static thermal permeability, Λ' is the characteristic size of the pores for thermal effects, and finally b' is a parameter which can provide minor modifications of the effective bulk modulus in the low- and medium-frequency range; the low-frequency limit α'_0 for the real part of α' (i.e., $\lim_{\omega\to 0}\mathrm{Re}\,\alpha' = \alpha'_0$) is achieved when

$$b' = \frac{2k'_0}{\Lambda'^2\phi(\alpha'_0 - 1)}. \tag{6}$$

Equations (1) and (4), together with the expressions (2) and (5), constitute a very effective model for sound propagation in porous media with a rigid frame (in fact, the JCAPL model). This model involves eight parameters which, in different ways, depend on the micro-geometry of the porous material (being, in fact, its average macroscopic properties); they are: ϕ, α_∞, k_0, k'_0, Λ, Λ', b (or α_0), and b' (or α'_0). However, by choosing to put $b = 1$, or in consequence, $\alpha_0 = \alpha_\infty + \frac{2\alpha_\infty^2 k_0}{\Lambda^2\phi}$, the simplified (original) Johnson's

model[7] for dynamic tortuosity is achieved. A similar simplification can be done for the Lafarge model[9] for thermal tortuosity by assuming that $b' = 1$, or $\alpha_0' = 1 + \frac{2k_0'}{\Lambda'^2\phi}$, thus, neglecting the possibility of some minor modifications in the low- and medium-frequency range. Eventually, a simplified version, i.e., the JCAL model, which involves only six geometrical parameters (ϕ, α_∞, k_0, k_0', Λ and Λ'), can be written as follows:

$$\begin{aligned} \alpha(\omega) &= \alpha_\infty + \frac{\nu_\mathrm{f}}{\mathrm{i}\omega}\frac{\phi}{k_0}\sqrt{\frac{\mathrm{i}\omega}{\nu_\mathrm{f}}\left(\frac{2\alpha_\infty k_0}{\Lambda\phi}\right)^2 + 1}, \\ \alpha'(\omega) &= 1 + \frac{\nu_\mathrm{f}'}{\mathrm{i}\omega}\frac{\phi}{k_0'}\sqrt{\frac{\mathrm{i}\omega}{\nu_\mathrm{f}'}\left(\frac{2k_0'}{\Lambda'\phi}\right)^2 + 1}. \end{aligned} \tag{7}$$

B. Surface impedance and acoustic absorption coefficient for double- and single-layered media

Figure 1 shows the configuration of a double-layered medium of thickness ℓ, set on a rigid wall and composed of an inner layer 1 with thickness $\ell_1 = \xi\ell$, where $\xi \in (0,1)$, and an outer layer 2 with thickness $\ell_2 = (1-\xi)\ell$. The densities of the materials of these layers are ϱ_1 and ϱ_2, respectively. In general, these materials may be porous with open porosities ϕ_1 for the inner layer, and ϕ_2 for the outer one. These porosities will be used in the formulas derived below, although in further considerations the layer 1 will be an air gap, which means that its porosity should be simply set to 1. A plane harmonic acoustic wave propagates in the fluid (i.e., the air, which also fills the pores in both layers) and penetrates at normal incidence into the double-layered medium. It passes both layers, and (provided that the two materials are different) it is partially reflected at the interface between the layers, and finally, it is fully reflected by the rigid wall. A standing-wave interference pattern results due to the superposition of forward- and backward-travelling waves. By measuring the sound pressure at two fixed locations outside the medium, it is possible to determine important acoustical characteristics of the two-layered arrangement, namely, the complex-valued normal acoustic impedance and reflection coefficient, and the real-valued sound absorption coefficient.

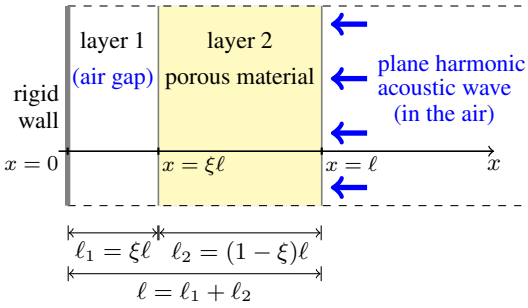

Figure 1: A two-layered medium: A layer of porous material with an air gap (or another material) close to the rigid wall

Assuming that the speed of sound (and therefore, the wave numbers) and the density in both materials are known, plane wave propagation in a double-layered medium is governed by the system of two Helmholtz equations, each valid for one of the two layers and coupled with the other equation only at the interface where the amplitudes of the pressure and velocity flux for both layers must be equal. This linear system of equations can be solved analytically.

Thus, the (complex amplitudes of) acoustic pressure and particle velocity in layer 1, that is, for $x \in [0, \xi\ell]$, are in fact given by the following formulas

$$p^{(1)}(x) = A_1^{(1)}\mathrm{e}^{-\mathrm{i}k_1 x} + A_2^{(1)}\mathrm{e}^{\mathrm{i}k_1 x}\,, \tag{8}$$

$$v^{(1)}(x) = \frac{k_1}{\omega\varrho_1}\left(A_1^{(1)}\mathrm{e}^{-\mathrm{i}k_1 x} - A_2^{(1)}\mathrm{e}^{\mathrm{i}k_1 x}\right), \tag{9}$$

where k_1 is the wave number in the medium of layer 1, while $A_1^{(1)}$ and $A_2^{(1)}$ are the (unknown) complex amplitudes of the incident and reflected pressure waves, respectively. Similarly, the wave number in medium 2 is denoted by k_2, the (unknown) pressure amplitudes of the incident and reflected waves in layer 2 are denoted by $A_1^{(2)}$ and $A_2^{(2)}$, respectively, and the formulas for acoustic pressure and particle velocity are

$$p^{(2)}(x) = A_1^{(2)}\mathrm{e}^{-\mathrm{i}k_2 x} + A_2^{(2)}\mathrm{e}^{\mathrm{i}k_2 x}\,, \tag{10}$$

$$v^{(2)}(x) = \frac{k_2}{\omega\varrho_2}\left(A_1^{(2)}\mathrm{e}^{-\mathrm{i}k_2 x} - A_2^{(2)}\mathrm{e}^{\mathrm{i}k_2 x}\right), \tag{11}$$

for $x \in [\xi\ell, \ell]$. In the case of porous layers $v^{(1)}$ and $v^{(2)}$ are in fact the effective velocity fluxes, so that the real fluid velocity in pores is $v^{(1)}/\phi_1$ or $v^{(2)}/\phi_2$, respectively.

In the proposed approach, the first layer will be the air gap so that $\phi_1 = 1$, $\varrho_1 = \varrho_\mathrm{f}$ and $k_1 = \omega/c_\mathrm{f}$, where ϱ_f and c_f are the density of air and the speed of sound in air, respectively. The second layer will be a layer of porous material with open porosity $\phi_2 = \phi \in (0,1)$ filled with air. Moreover, for this layer $\varrho_2 = \varrho(\omega)$ and $k_2 = \omega/c(\omega)$, where the effective density $\varrho(\omega)$ and the effective speed of sound $c(\omega)$ for the porous material are not real-valued constants, but are complex frequency-dependent characteristics defined by the formulas presented in Section A.

The unknown amplitudes of the pressure waves are derived by applying the boundary and interface conditions, namely:

- the zero normal velocity at the rigid wall, i.e., at $x = 0$: $v^{(1)}(0) = 0$;
- the pressure and velocity flux continuity at the interface between two layers, i.e., at $x = \xi\ell$: $p^{(1)}(\xi\ell) = p^{(2)}(\xi\ell)$ and $v^{(1)}(\xi\ell) = v^{(2)}(\xi\ell)$;
- the pressure boundary condition at the free surface, i.e., at $x = \ell$: $p^{(2)}(\ell) = \hat{p}$, where $\hat{p}$ is the acoustic pressure amplitude of the incident plane harmonic wave penetrating the two-layered medium.

Eventually, after introducing the following notations,

$$\begin{aligned} \kappa_1 &= \mathrm{i}k_1\ell\,, & \kappa_2 &= \mathrm{i}k_2\ell\,, \\ B_1 &= k_2\varrho_1 + k_1\varrho_2\,, & B_2 &= k_2\varrho_1 - k_1\varrho_2\,, \end{aligned} \tag{12}$$

the expressions for complex amplitudes are

$$A_1^{(1)} = A_2^{(1)} = \hat{p}\frac{(B_1+B_2)\mathrm{e}^{\xi\kappa_1+(1+\xi)\kappa_2}}{A_0}\,, \tag{13}$$

$$A_1^{(2)} = \hat{p}\frac{B_1\mathrm{e}^{(1+2\xi)\kappa_2} + B_2\mathrm{e}^{2\xi\kappa_1+(1+2\xi)\kappa_2}}{A_0}\,, \tag{14}$$

$$A_2^{(2)} = \hat{p}\frac{B_1\mathrm{e}^{2\xi\kappa_1+\kappa_2} + B_2\mathrm{e}^{\kappa_2}}{A_0}\,, \tag{15}$$

where the denominator equals

$$A_0 = B_1\left(\mathrm{e}^{2\xi\kappa_2} + \mathrm{e}^{2(\xi\kappa_1+\kappa_2)}\right) + B_2\left(\mathrm{e}^{2\kappa_2} + \mathrm{e}^{2\xi(\kappa_1+\kappa_2)}\right). \quad (16)$$

Now, the surface acoustic impedance at the free surface of two-layered medium, i.e., at $x = \ell$, can be computed as

$$Z = \frac{p^{(2)}(\ell)}{-v^{(2)}(\ell)} = \frac{\omega\varrho_2}{k_2}\left[-\frac{A_1^{(2)}}{\hat{p}}\mathrm{e}^{-\mathrm{i}k_2\ell} + \frac{A_2^{(2)}}{\hat{p}}\mathrm{e}^{\mathrm{i}k_2\ell}\right]^{-1}, \quad (17)$$

where $p^{(2)}(\ell) = \hat{p}$ and the coefficients $A_1^{(2)}/\hat{p}$ and $A_2^{(2)}/\hat{p}$ are calculated from the formulas derived above, and it should be noted that the surface impedance $Z(\omega)$ is a complex-valued frequency-dependent characteristics which actually does not depend on the excitation pressure amplitude $\hat{p}$.

When there is no air gap (or inner layer), and a single porous layer of thickness ℓ is set directly on the rigid wall (that is for $\xi = 0$, $\ell_1 = 0$, and $\ell_2 = \ell$), the whole problem is simplified. This is in fact a typical configuration used in standard material testing. Then, the surface acoustic impedance of single porous layer is

$$\begin{aligned} Z &= \varrho c\frac{\exp(2\mathrm{i}\omega\ell/c)+1}{\exp(2\mathrm{i}\omega\ell/c)-1} = -\mathrm{i}\varrho c\cot\left(\frac{\omega\ell}{c}\right) \\ &= -\frac{\mathrm{i}Z_\mathrm{f}}{\phi}\sqrt{\frac{\alpha}{\beta}}\cot\left(\frac{\omega\ell}{c_\mathrm{f}}\sqrt{\alpha\beta}\right), \end{aligned} \quad (18)$$

where $Z_\mathrm{f} = \varrho_\mathrm{f} c_\mathrm{f}$ is the characteristic impedance of the fluid (air) in the pores and outside the porous medium, and the frequency-dependent functions $\alpha(\omega)$ and $\beta(\omega)$ (or the effective quantities $\varrho(\omega)$ and $c(\omega)$) are computed using formulas from Section A.

Whatever the case, when the surface acoustic impedance of a two-layered (17) or single-layer medium (18) is known, the complex-valued reflection coefficient R and the real-valued acoustic absorption coefficient A can be calculated [12,16] as

$$R(\omega) = \frac{Z(\omega) - Z_\mathrm{f}}{Z(\omega) + Z_\mathrm{f}}, \qquad A(\omega) = 1 - |R(\omega)|^2. \quad (19)$$

The surface acoustic impedance (17) or (18), as well as the reflection and absorption coefficients (19) can be determined experimentally in an impedance tube in some frequency range (which depends on the size of the sample and the tube), using the so-called two-microphone transfer function method [38–40].

III. PROCEDURE FOR INVERSE PARAMETRIC IDENTIFICATION OF RIGID PORO-ACOUSTICAL MODEL

A. A normalized set of dimensionless parameters

A method for the parameter identification for the rigid-porous model, based on some acoustical measurements, will now be presented. For this purpose, a set of six dimensionless parameters, which are in an unequivocal relation with the JCAL model parameters and should render the optimization algorithm robust, is proposed as follows:

$$\begin{aligned} &p_0 = \phi, \quad p_1 = \alpha_\infty - 1, \quad p_2 = \frac{\nu_\mathrm{f}}{\omega_*}\frac{\phi}{k_0}, \quad p_3 = \frac{\nu'_\mathrm{f}}{\omega'_*}\frac{\phi}{k'_0}, \\ &p_4 = \frac{\omega_*}{\nu_\mathrm{f}}\left(\frac{2\alpha_\infty k_0}{\Lambda\phi}\right)^2, \quad p_5 = \frac{\omega'_*}{\nu'_\mathrm{f}}\left(\frac{2k'_0}{\Lambda'\phi}\right)^2, \end{aligned} \quad (20)$$

with two additional dimensionless parameters in the case of the JCAPL model:

$$p_6 = b = \frac{2\alpha_\infty^2 k_0}{\Lambda^2\phi(\alpha_0 - \alpha_\infty)}, \quad p_7 = b' = \frac{2k'_0}{\Lambda'^2\phi(\alpha'_0 - 1)}. \quad (21)$$

Here, the definitions of the parameters $p_2,\ldots,p_5$ involve the angular frequencies $\omega_* = 2\pi f_*$ and $\omega'_* = 2\pi f'_*$, where f_* and f'_* are some arbitrarily chosen scaling (normalizing) frequencies for viscous and thermal dissipation effects, respectively. They may be related to the critical frequencies delimiting the low- and high-frequency regimes of viscous and thermal effects. It is important to emphasize that the scaling frequencies are not additional parameters since they can be chosen quite arbitrarily, and for various choices, the same results for the model parameters should be obtained [35], although the corresponding sets of the scaled dimensionless parameters will be obviously different. Nevertheless, reasonable values for these frequencies must be used (see examples in this work) in order to make the identification procedure successful. As a matter of fact, the scaling frequencies allow properly normalizing the vector of dimensionless parameters. The main purpose is that for the same initial value (typically 1) used for those parameters by the optimization procedure, when the identification is completed, the found values of the dimensionless parameters should be of more or less similar order.

Now, the formulas for the dynamic viscous and thermal tortuosities, α and α', can be rewritten in the following form:

$$\begin{aligned} \alpha(\omega) &= 1 + p_1 + \frac{\omega_*}{\mathrm{i}\omega}p_2\left[\sqrt{\frac{\mathrm{i}\omega}{\omega_*}p_4 + p_6^2} - p_6 + 1\right], \\ \alpha'(\omega) &= 1 + \frac{\omega'_*}{\mathrm{i}\omega}p_3\left[\sqrt{\frac{\mathrm{i}\omega}{\omega'_*}p_5 + p_7^2} - p_7 + 1\right]. \end{aligned} \quad (22)$$

It should be observed that the dimensionless parameter p_0 is not present in these formulas. It is actually the total open porosity parameter ϕ, which in the model formulas for the dynamic tortuosities (2) and (5), or (7) (as well as in the definitions for parameters $p_2,\ldots,p_7$), appears always in rational relation with the permeabilities k_0 or k'_0. Nevertheless, the parameter $p_0 = \phi$ must be included in the proposed set of identifiable parameters, because the porosity occurs independently (of k_0 and k'_0) in the formulas for surface impedance (17) or (18) which will be used by the identification procedure.

After the dimensionless parameters have been found, the model parameters can be calculated as follows:

$$\begin{aligned} &\phi = p_0, \quad \alpha_\infty = 1 + p_1, \quad k_0 = \frac{\nu_\mathrm{f}}{\omega_*}\frac{\phi}{p_2}, \quad k'_0 = \frac{\nu'_\mathrm{f}}{\omega'_*}\frac{\phi}{p_3}, \\ &\Lambda = \frac{2+2p_1}{p_2}\sqrt{\frac{\nu_\mathrm{f}}{\omega_* p_4}}, \quad \Lambda' = \frac{2}{p_3}\sqrt{\frac{\nu'_\mathrm{f}}{\omega'_* p_5}}, \end{aligned} \quad (23)$$

and furthermore, for the JCAPL version of the model:

$$\alpha_0 = 1 + p_1 + \frac{p_2 p_4}{2p_6}, \quad \alpha'_0 = 1 + \frac{p_3 p_5}{2p_7}, \quad (24)$$

In the case of the JCAL model (7), only six dimensionless parameters (20) (and so only six model parameters (23)) need to be identified (since $p_6 = b = 1$ and $p_7 = b' = 1$) and in that case the

formulas for the dynamic tortuosities are

$$\alpha(\omega) = 1 + p_1 + \frac{\omega_*}{\mathrm{i}\omega} p_2 \sqrt{\frac{\mathrm{i}\omega}{\omega_*} p_4 + 1},$$
$$\alpha'(\omega) = 1 + \frac{\omega'_*}{\mathrm{i}\omega} p_3 \sqrt{\frac{\mathrm{i}\omega}{\omega'_*} p_5 + 1}. \tag{25}$$

B. The objective function and identification procedure

Over some frequency range, the surface impedance of a sample of porous material of known thickness is measured in an impedance tube. As a matter of fact, a few measurements are carried out for the same sample set directly on the rigid termination in the tube and with air gaps of various (known) thicknesses between the sample and the rigid termination.

The objective function is defined as the sum of squared measures of the difference between the experimental curves (i.e., the real and imaginary parts of the measured surface impedances) and their analytical analogues computed from the model discussed above, with some assumed values for the dimensionless parameters; namely:

$$\begin{aligned} F(\mathbf{p}) &= \sum_m \sum_\omega \left| Z_m(\omega;\mathbf{p}) - Z_m^{\mathrm{exp}}(\omega) \right|^2 \\ &= \sum_m \sum_\omega \Big[\big(\mathrm{Re}\, Z_m(\omega;\mathbf{p}) - \mathrm{Re}\, Z_m^{\mathrm{exp}}(\omega) \big)^2 \\ &\quad + \big(\mathrm{Im}\, Z_m(\omega;\mathbf{p}) - \mathrm{Im}\, Z_m^{\mathrm{exp}}(\omega) \big)^2 \Big]. \end{aligned} \tag{26}$$

Here: $\mathbf{p}$ is the vector of dimensionless parameters with six components defined by (20) – in the case of the standard JCAL model – or with eight components defined by formulas (20) and (21) – in the case of the enhanced JCAPL model; $Z_m^{\mathrm{exp}}(\omega)$ is the acoustic impedance measured at frequency ω for the measurement case m, and $Z_m(\omega;\mathbf{p})$ is its computed counterpart; the summation ($\sum_\omega$) is carried out over the discrete set of measurement/computational frequencies ω (from the relevant frequency range), as well as over all the measurement cases ($\sum_m$) with various known air gaps (or with the sample set directly on the rigid termination). The acoustic impedance values are computed using formulas (17) or (18) with ϕ substituted by p_0 and the porous layer effective quantities $\varrho(\omega;\mathbf{p})$ and $c(\omega;\mathbf{p})$ calculated from the model formulas where the viscous and thermal tortuosities are determined with respect to the dimensionless parameters, that is, from Equation (25) for the JCAL case, or Equation (22) in the JCAPL case. The analytical formulas for the gradient of the objective function with respect to the parameters $\mathbf{p}$ can be derived (see the Appendix) to be used by minimization procedures.

During the identification procedure, the objective function is minimized with respect to the dimensionless parameters $\mathbf{p}$. It is required that all the parameters are positive, however, some additional constraints may be imposed. For example, it is known that thermal dissipation effects are associated with the so-called thermal skin depth, which tends to be bigger than the viscous skin depth corresponding to the viscous dissipation effects. Thus, the thermal effects are rather associated with the the pore size, while the viscous effects are associated with the size of the "windows" (and small pores) linking the pores; therefore, in general, the viscous and thermal characteristic lengths should satisfy the following relation $\Lambda \leqslant \Lambda'$. Similarly, one may always expect that $k_0 \leqslant k'_0$, which means that $p_3 \leqslant \frac{\omega_*}{\omega'_* \mathrm{Pr}} p_2$. Nevertheless, the optimization algorithms with (simple) positive-value constraints (or even algorithms without constraints) can be successfully used for the correct identification of the model parameters, thanks to the normalization realized by the scaling frequencies. The initial values for the components of the vector $\mathbf{p}$ should be all set to 1, and the reference frequencies, f_* and f'_*, may be chosen with some reasonable freedom (though, rather $f_* > f'_*$).

Mathematically speaking, the inverse characterization uses the least squares method: a numerical model is fitted to experimental data by minimizing a quadratic function of the differences between the data and their model counterpart. The modeled problem is of the steady-state kind (its behavior does not depend on any initial conditions and it continues into the future). An inverse solution exists because the model function is continuous in its parameters with bounded domains. Since many experimental curves are suggested to be used simultaneously in the error minimization, the least square problem is overdetermined, and it seems that the solution is unique. Thus, the problem is rather well-posed[41], however, the problem's different sensitivity to various parameters[42] may imply ill-conditioning. An important role in fitting models to measurements is often played by the Hessian matrix which contains the second derivatives of the quadratic objective function[43]. In the discussed method, the formulas for the normalized parameters set at once the conditioning of the fitting-error minimization problem at a better level, and a good choice of the normalizing frequencies improves it by reducing the condition number of the Hessian matrix.

IV. EXAMPLE BASED ON A NUMERICAL EXPERIMENT

The following numerical experiment was carried out. First, each value from a set of realistic parameters for the six-parameter JCAL model of a rigid porous medium – listed in Table I as the original values – was subject to some random deviation. As a matter of fact, for each parameter, three different random deviations were independently effectuated. The results are presented in Table I as the A-, B-, and C-deviated values. The average deviated values, computed for each parameter as the arithmetic mean from the corresponding A-, B- and C-deviations, are also listed in Table I, whereas in Figure 2 the relative difference of each deviated value from its original is shown. It should be noted that the A-, B-, and C-deviated values differ from their original counterparts from by several percent to nearly 20%, however, the average deviation tends rather to be a few percent (less than 6%) for each parameter.

Table I: Values of transport parameters

Parameter value↓ [unit]	ϕ [%]	α_∞ [–]	k_0 [10^{-9}m^2]	k'_0	Λ [10^{-6}m]	Λ'
original:	88.00	1.800	0.500	2.000	50.00	180.0
A-deviated:	81.63	1.789	0.516	1.823	58.54	173.2
B-deviated:	82.79	1.690	0.539	1.914	54.42	158.4
C-deviated:	93.50	1.840	0.509	1.920	43.15	213.8
averaged:	85.97	1.760	0.521	1.886	52.04	181.8
identified:	86.06	1.739	0.508	1.840	50.99	197.6

The A-, B-, and C-deviated values of the JCAL model parameters were used in modelling calculations to produce artificial experimental curves of surface acoustic impedance for three configuration cases of a 30 mm-thick rigid porous layer: (a) a porous layer described by the A-deviated values of model parameters set

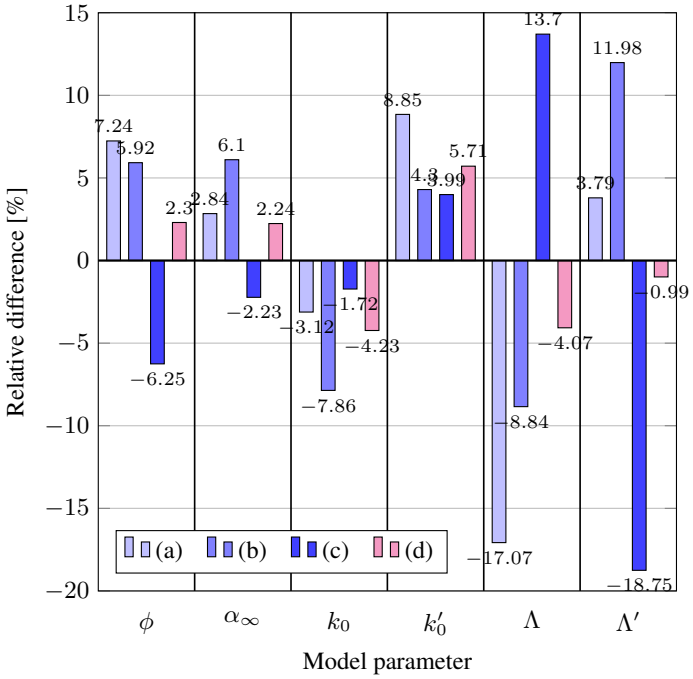

Figure 2: Relative differences of the deviated values of model parameters from their original values: (a) A-deviation, (b) B-deviation, (c) C-deviation, (d) average deviation, i.e., the arithmetic mean value from the corresponding A-, B- and C-deviated values

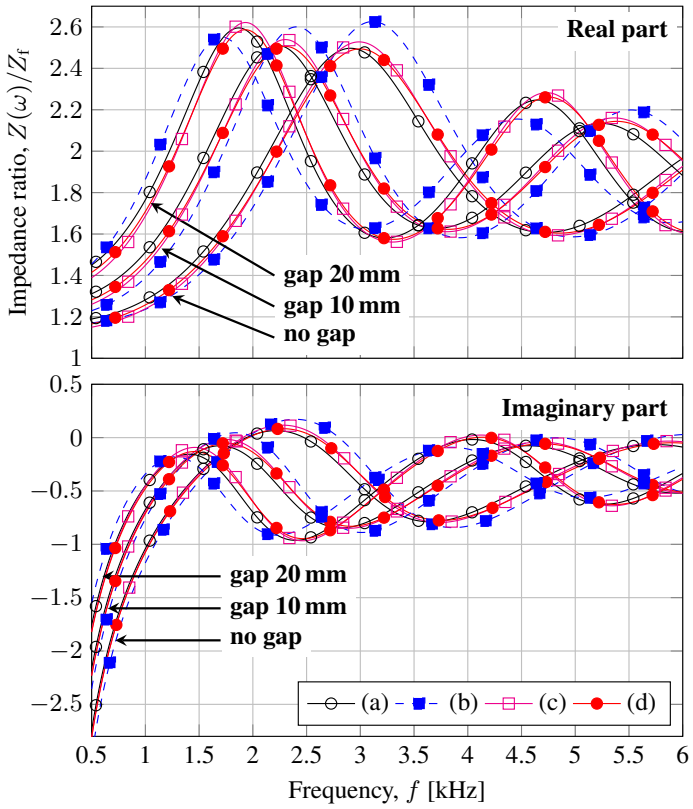

Figure 3: Surface acoustic impedance (its ratio to the characteristic impedance of air Z_f) of the 30 mm-thick porous layer set directly on the rigid wall, or with the 10 mm or 20 mm-thick air gaps between the layer and the wall, computed for the following values of model parameters (see Table I): (a) original, (b) A-deviated – for the no-gap case, B-deviated – for gap 10 mm, or C-deviated – for gap 20 mm, (c) averaged, (d) identified

directly to the rigid wall, (b) the porous layer described by the B-deviated values of model parameters set with a 10 mm-thick air gap to the rigid wall, and (c) the porous layer described by the C-deviated values of model parameters set with a 20 mm-thick air gap to the rigid wall. The results obtained in this way, i.e., from the deviated values of the parameters, can therefore be considered as realistic results vitiated by measurement errors or some imperfections (local inhomogeneities) of real samples. These impedance curves are plotted in Figure 3 as curves (b). For comparison, the curves computed from the original values of the model parameters, as well as from the averaged-deviation values, are also shown as curves (a) and (c), respectively. Nevertheless, one must remember that only these A-, B-, and C-deviated curves were used by the identification procedure, which eventually provided the identified values of the model parameters listed in the bottom line of Table I. The corresponding impedance curves were also computed for these identified values, and are presented in Figure 3 as curves (d). It is clearly visible that in each case they are the ones closest to the curves obtained from the averaged-deviation parameters, although, as mentioned already above, those latter were not used by the identification procedure. Nevertheless, the overall differences between the various corresponding curves are rather small, which illustrates the fact that such moderate variations of model parameters tend to produce quite similar results.

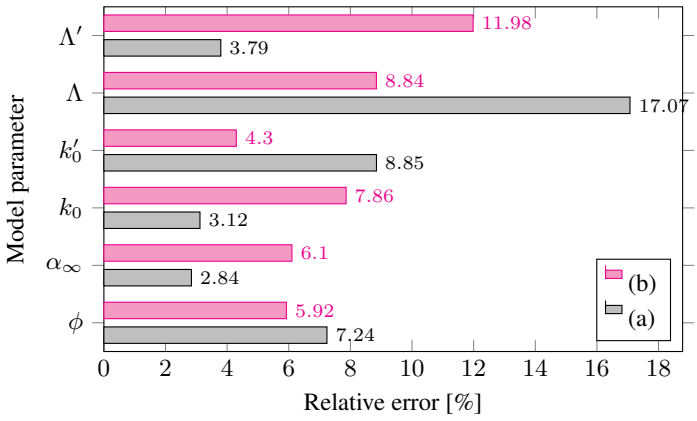

Figure 4: Relative errors of the identified parameters with respect to the corresponding: (a) original values, (b) averaged-deviation values

Figure 4 shows the relative errors for each identified parameter with respect to its original value and the averaged-deviation value. The errors with respect to the average-deviations vary from about 4% to 12%, whereas the errors with respect to the original values are more dispersed: they are from about 3% to 17%. One should remember, however, that for another numerical test of this type (i.e., another set of random deviations), the errors would be (slightly) different. Nevertheless, it was checked that the mean error tend to be smaller when the identified parameters are compared with the average-deviation values. Finally, the curves of the acoustic absorption coefficient computed for all three configurations of a porous layer (i.e., with or without air gaps) for the JCAL model with original, deviated and identified parameters are presented in Figure 5. Again, the curves computed from the identified model are closest to the results calculated using the parameters with average-deviation (although the identification procedure used jointly the A-, B-, and C-deviated curves of surface acoustic impedance).

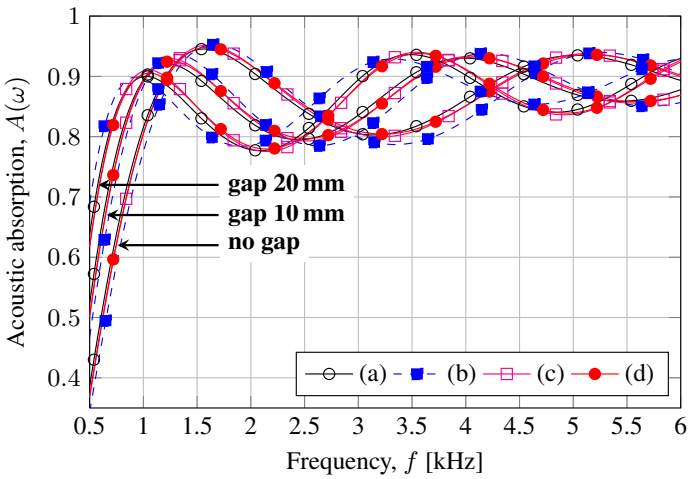

Figure 5: Acoustic absorption coefficients for the 30 mm-thick porous layer set directly on the rigid wall, or with 10 mm or 20 mm-thick air gaps between the layer and the wall – see Figure 3 for the description of curve denotations

V. EXPERIMENTAL VALIDATION OF THE INVERSE CHARACTERIZATION PROCEDURE

A. Inverse characterization of a ceramic foam

The characterization procedure was applied to two kinds of porous foams – see Figure 6. First, it was a ceramic (aluminium oxide) foam of a relatively high open porosity[44]. It has been recently reported that such foams have a very complex micro-geometry and exhibit good sound absorbing properties[45,46]. From two specimens of such foam manufactured separately, one with thickness app. 24 mm, the other with thickness app. 18 mm, two cylindrical samples were cut with a diameter of 29 mm (see Figure 6) to be well-fitted inside an impedance tube. Both samples were measured in the tube for their surface acoustic impedance and absorption coefficient in the frequency range from 500 Hz to 6 kHz, using the so-called two-microphone transfer function method[38,47,48]. Each of the samples was tested in five configurations: first, set directly to the rigid piston termination in the tube, and then with air gaps between the sample and the rigid termination so that the total thickness of the two-layered sound absorbing medium was 30, 40, 50, and 60 mm, respectively.

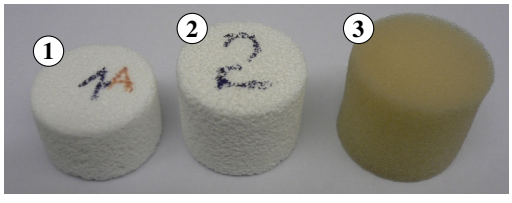

Figure 6: Two cylindrical porous ceramic (alumina) samples with diameter 29 mm and thickness (height): (1) 18 mm, (2) 24 mm, and (3) a sample of PU foam with thickness 26 mm

The impedance curves measured for the thicker sample were used by the parametric identification algorithm. Their real and imaginary parts are shown in Figure 7 (as the ratio to the characteristic impedance of air Z_f) together with the corresponding curves calculated after the identification was accomplished from the analytical JCAL model using the identified parameters – for the sake of legibility the results for only three configurations are presented, namely: for the case with no gap, and for the total thicknesses of 40 mm and 60 mm.

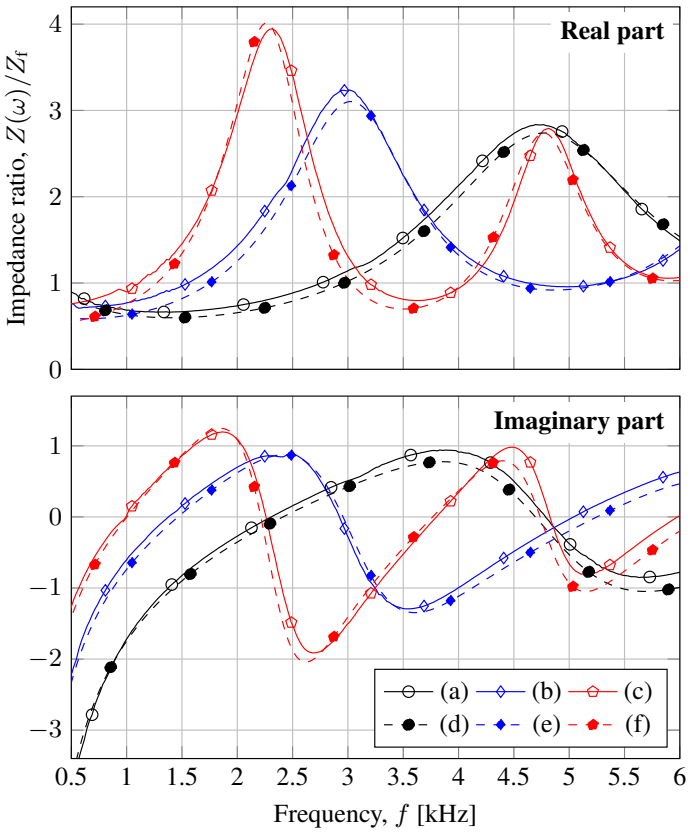

Figure 7: Surface acoustic impedance ratio for the 24 mm-thick porous ceramic sample with or without an air gap to the rigid wall, and the total thickness (sample+gap): (a,d) equal to the thickness of ceramic sample, i.e., no gap, (b,e) 40 mm, (c,f) 60 mm. The results of the experimental testing (a,b,c) and modeling (d,e,f) using the identified parameters

Table II: Identified values of transport parameters for porous ceramic sample

Parameter	Symbol	Unit	Identified value
porosity	ϕ	%	89.75
tortuosity	α_∞	–	1.234
viscous permeability	k_0	$10^{-9}\mathrm{m}^2$	2.275
thermal permeability	k_0'	$10^{-9}\mathrm{m}^2$	4.799
viscous length	Λ	$10^{-6}\mathrm{m}$	51.84
thermal length	Λ'	$10^{-6}\mathrm{m}$	333.0

The geometric parameters identified by the error-minimization procedure are listed in Table II and their corresponding dimensionless parameters, obtained by means of the scaling frequencies $f_* = 700$ Hz and $f_*' = 500$ Hz, are shown in Figure 8. It should be noted that the identified porosity of about 90% is in excellent accordance with the value declared by the foam manufacturer[44]. Finally, some of the acoustic absorption curves measured in an impedance tube and computed from the model are presented in Figure 9 for the identified porous sample with thickness 24 mm.

For further verification, the parameters identified from the impedance curves measured for the 24 mm-thick porous sample were also used to estimate the surface acoustic impedance and absorption for the second sample, of presumably the same porous

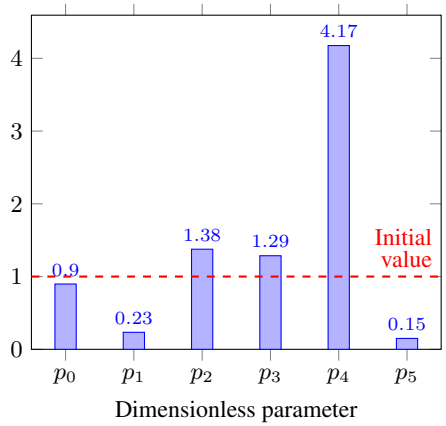

Figure 8: Identified values of dimensionless parameters (for alumina ceramics)

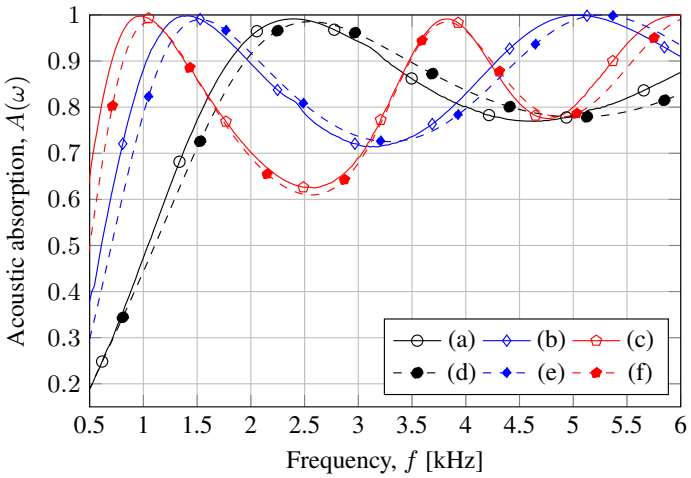

Figure 9: Acoustic absorption coefficient for the 24 mm-thick porous ceramic sample in various configurations (see caption to Figure 7). The results of the experimental testing (a,b,c) and modeling (d,e,f) using the identified parameters

ceramics yet with a thickness of 18 mm. In Figures 10 and 11 these results, calculated for three configurations with (or without) various air gaps, are compared with the relevant measurements. Here, the discrepancies between the measured and modeling results are bigger, probably because of the poor quality of one face of this sample; however, one should also recall that the samples were cut from two separate specimens, which had been manufactured independently even though using the same technology (which involved semi-manual mixing). Nevertheless, the general agreement between the corresponding curves is rather good, which essentially validates the identification.

B. Inverse characterization of a polyurethane foam

A polyurethane foam was used for the second test of the inverse characterization procedure. The sample of PU foam with thickness 26 mm (see Figure 6) was measured in the impedance tube in five configurations: set directly on the rigid termination in the tube or with such air gaps so that the total thicknesses were 40 mm, 60 mm, 80 mm, and 100 mm. The foam was sufficiently stiff, which justified the rigid-frame assumption and the characterization procedure based on the JCAL model was carried out using the surface impedance measurements.

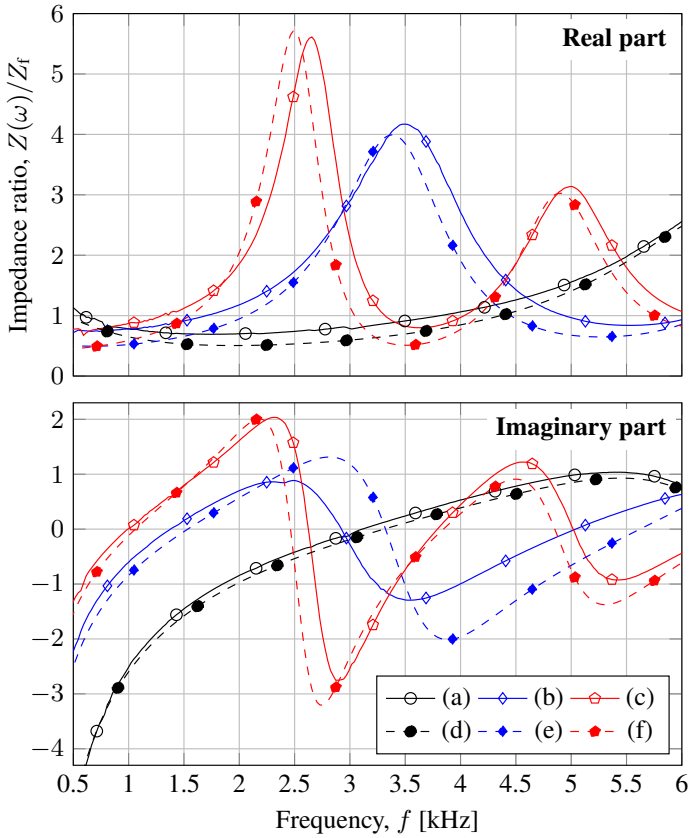

Figure 10: Surface acoustic impedance ratio for the 18 mm-thick porous ceramic sample in various configurations (see caption to Figure 7). The results of the experimental testing (a,b,c) and modeling (d,e,f) using the parameters identified for the sample 24 mm-thick

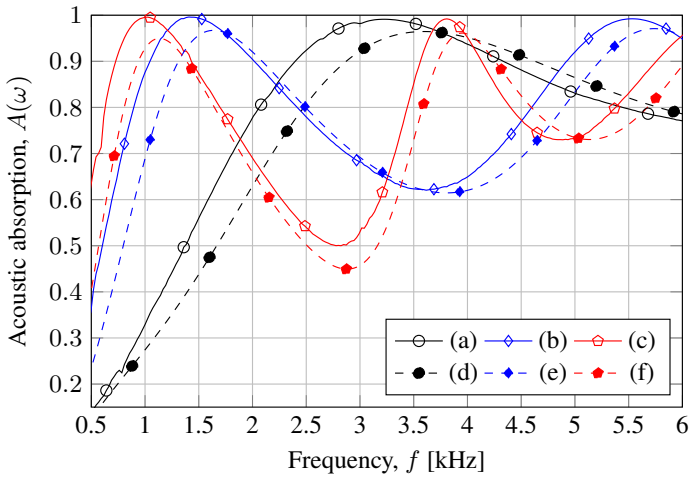

Figure 11: Acoustic absorption coefficient for the 18 mm-thick porous ceramic sample in various configurations (see caption to Figure 7). The results of the experimental testing (a,b,c) and modeling (d,e,f) using the parameters identified for the sample 24 mm-thick

In order to illustrate the effect of the proposed normalizing frequencies, f_* and f'_*, three solutions for the normalized dimensionless parameters are shown in Figure 12; they were obtained for three sets of normalizing frequencies, namely: (1) for $f_* = 3\,\text{kHz}$ and $f'_* = 2\,\text{kHz}$; (2) for $f_* = 2\,\text{kHz}$ and $f'_* = 500\,\text{Hz}$; (3) for $f_* = 400\,\text{Hz}$ and $f'_* = 300\,\text{Hz}$. One should note that the parameters p_0 and p_1 are (respectively) the same in all solutions presented in Figure 12, since they do not depend on the normalizing

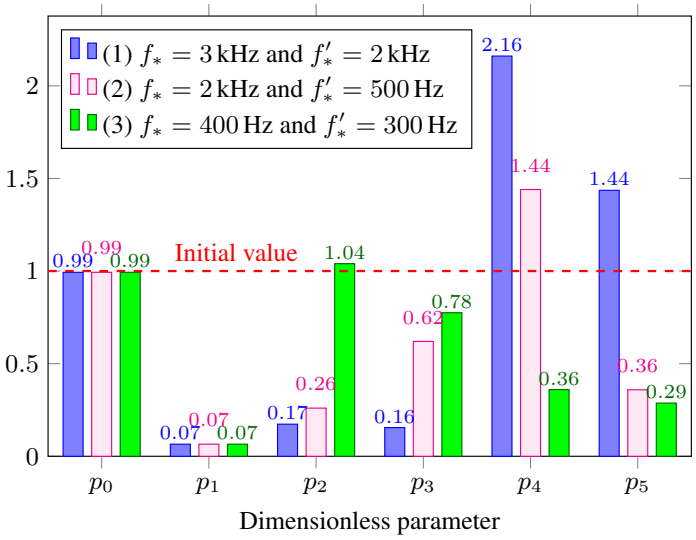

Figure 12: Identified values of dimensionless parameters for the PU sample: three cases for various normalizing frequencies

frequencies. On the other hand, the identified values of all other parameters, i.e., p_2, p_3, p_4 and p_5, are different between the solutions, since they depend on the normalizing frequencies. Another observation: the most dispersed dimensionless parameters are for the case (1), while the most compact is the dimensionless vector found for the case (3). However, what is important, after using the formulas for the model parameters (23), the results are the same, at least up to the three significant figures of each number, which are presented in the last column of Table III. Here, the corresponding "initial" values of the model parameters are also given, for the all three choices, (1), (2) and (3), of the normalizing frequencies. Obviously, the identification procedure directly identifies only the normalized parameters $p_0, \ldots, p_5$, and the important feature of the method is that the initial values for all of them is 1. Therefore, the "initial" values for the model parameters are not used by any minimization procedure, but they are simply calculated here from the unit values of the normalized parameters and the chosen normalizing frequencies. Again, since these frequencies do not affect p_0 and p_1 which unequivocally and directly define ϕ and α_∞, those two model parameters have the same "initial" values whatever was the choice for the normalizing frequencies; the other "initial" values are different. One may observe that the "initial" value for the viscous length is higher than the "initial" value of the thermal length, however, their final identified values are more properly related: the thermal length is nearly twice as large as the viscous one. When the "initial" values are compared with the identified ones, the case (3) has the closest results, whereas the largest differences are for the case (1). One may conclude that a better choice of the normalizing frequencies puts the unit initial values of the dimensionless parameters closer to the values which render the minimum of the objective function.

The Hessian matrix of the objective function was computed for three identified vectors of normalized parameters. In accordance with the previous observations, it was found that the conditioned number of the Hessian matrix computed in the case (3) was 36 times smaller than for the worst normalization case (1). Thus, one may conclude that a better choice of normalizing frequencies improves the conditioning of the Hessian matrix of the objective function. Nevertheless, for this PU foam the inverse characterization

Table III: "Initial" and identified values of transport parameters for PU foam

Parameter	Symbol	Unit	"Initial" value (1)	(2)	(3)	Ident.
porosity	ϕ	%	100	100	100	99.3
tortuosity	α_∞	–	2.00	2.00	2.00	1.07
viscous perm.	k_0	$10^{-9}\mathrm{m}^2$	0.82	1.24	4.94	4.72
thermal perm.	k'_0	$10^{-9}\mathrm{m}^2$	1.74	3.48	8.70	11.1
viscous length	Λ	$10^{-6}\mathrm{m}$	115	141	281	240
thermal length	Λ'	$10^{-6}\mathrm{m}$	83	118	187	449

procedure was very stable: the same results were obtained whatever the choice of normalizing frequencies. Figure 13 compares the acoustic absorption curves obtained from some measurements in the impedance tube with the corresponding curves calculated from the identified model parameters – the discrepancies are very small.

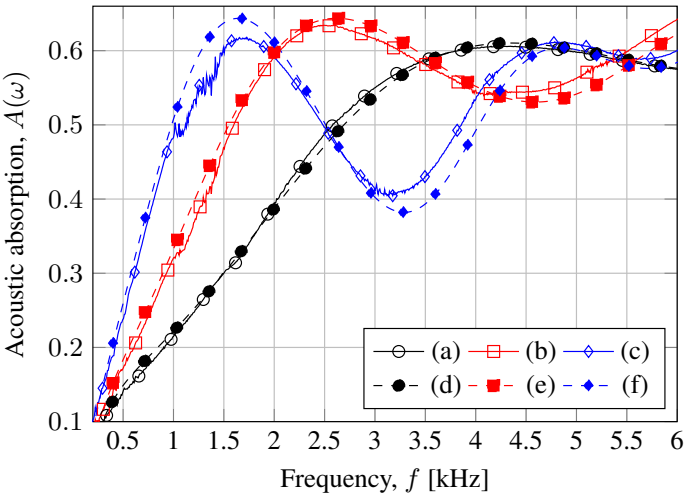

Figure 13: Acoustic absorption coefficient for the 26 mm-thick PU foam sample with or without an air gap to the rigid wall, and the total thickness (sample+gap): (a,d) equal to the thickness of PU sample, i.e., no gap, (b,e) 40 mm, (c,f) 60 mm. The results of the experimental testing (a,b,c) and modelling (d,e,f) using the identified parameters

The identified value of high porosity (see Table III) is typical for open-cell PU foams. Also typical is the identified viscous permeability (see Refs.[49,50]), which sets the value of the air flow resistivity to $3871\,\mathrm{Pa{\cdot}s/m^2}$ (the air flow resistivity for open-cell PU foams varies with their density, but is in the region of 2000 to $8000\,\mathrm{Pa{\cdot}s/m^2}$ for the densities of 20 to $60\,\mathrm{kg/m^3}$).

VI. CONCLUSIONS

A methodology for inverse parametric identification of rigid porous media on the basis of surface acoustic impedance measurements was discussed. The identification procedure applies the least squares method to fit the measurement curves with the results calculated analytically from the Johnson–Allard models[12]. In this way, important transport parameters may be simultaneously identified, in particular: the open porosity, tortuosity, viscous and thermal permeabilities, and two characteristic lengths. However, these model parameters are not directly sought for; instead, the identification algorithm minimizes the discrepancy between the experimental and analytical results with respect to a set of normalized

dimensionless parameters, which are in unequivocal relation to the model parameters. The proposed formulas of relation involve two scaling factors: the normalizing frequencies which may be related to the critical frequencies delimiting low- and high-frequency regimes of viscous and thermal effects. These scaling factors must be set beforehand, and they simply normalize the identification algorithm, which means that for various choices the identified sets of dimensionless parameters will differ merely in how they render the same (or very similar) values of the model parameters. In practice, the choice of scaling frequencies may slightly affect the identification errors, and it will certainly have an impact on the number of iterations needed by the minimization algorithm. Nevertheless, the choice of normalizing frequencies may be quite arbitrary, within some reasonable limits. It is also suggested that the thermal scaling frequency should be less than its viscous counterpart. The purpose for these scaling factors is that the order of the identified dimensionless parameters should be similar (as a matter of fact, in cases when they vary significantly, another choice of scaling frequencies should be tried). Moreover, the initial values for all dimensionless parameters may be simply set to 1 (thus, the corresponding initial values of model parameters will depend only on the two scaling frequencies). This is an important feature of the identification procedure: with a simple choice of initial values the iterative minimization should lead to the global minimum. Such approach should improve the robustness of the methodology which, however, depends most of all on the quality of experimental data. Therefore, the parametric identification should be effectuated with respect to many experimentally determined curves of acoustic impedance measured for the same porous material. This may be achieved by testing a few samples of various thickness in several configurations, namely, in the standard one – when a sample is set directly to the rigid termination in an impedance tube – and in double-layered arrangements with air gaps of known thickness between the sample and the rigid termination. The methodology was tested on data obtained from one numerical experiment as well as data from the measurements of two samples (of various thicknesses) of high-porosity alumina foam, and a sample of polyurethane foam, carried out in an impedance tube. The tests essentially validated the method, however, they also revealed a moderate accuracy (reliability) of identification because of a rather limited sensitivity of the impedance curves to some not very large variations of some of the model parameters (see also Ouisse *et al.*[42]).

ACKNOWLEDGEMENTS

The author wishes to express his sincere gratitude to Dr. Marek Potoczek from the Rzeszów University of Technology for providing two samples of porous ceramics. Financial support through the project "Modern Material Technologies in Aerospace Industry," No. POIG.01.01.02-00-015/08, is gratefully acknowledged. The dissemination of this work was supported through the FP7 EU project Smart-Nest (PIAPP-GA-2011-28499).

APPENDIX: GRADIENT OF THE OBJECTIVE FUNCTION

Here, the analytical formulas will be given for the gradient of the objective function defined with respect to one measurement configuration (i.e., $m = 1$ in the formula (26)), when a porous sample is set directly on the rigid wall (i.e., for $\ell_1 = 0$ and $\ell_2 = \ell$). In that case, the gradient components with respect to the (real-valued) parameters p_n ($n = 0, 1, \ldots, 5$) are:

$$\frac{\partial F(\mathbf{p})}{\partial p_n} = 2\sum_{\omega}\Big(\operatorname{Re} Z(\omega;\mathbf{p}) - \operatorname{Re} Z^{\exp}(\omega)\Big)\operatorname{Re}\frac{\partial Z(\omega;\mathbf{p})}{\partial p_n} + 2\sum_{\omega}\Big(\operatorname{Im} Z(\omega;\mathbf{p}) - \operatorname{Im} Z^{\exp}(\omega)\Big)\operatorname{Im}\frac{\partial Z(\omega;\mathbf{p})}{\partial p_n}\,.$$

where the components of the corresponding gradient of the surface acoustic impedance,

$$Z(\omega;\mathbf{p}) = -\frac{\mathrm{i}Z_{\mathrm{f}}}{p_0}\sqrt{\frac{\alpha(\omega;p_1,p_2,p_4)}{\beta\big(\alpha'(\omega;p_3,p_5)\big)}}\cot\Big(\frac{\omega\ell}{c_{\mathrm{f}}}\sqrt{\alpha(\ldots)\beta(\ldots)}\Big),$$

are computed as follows:

$$\frac{\partial Z}{\partial p_0} = -\frac{Z}{p_0}\,,\qquad \frac{\partial Z}{\partial p_1} = \frac{\partial Z}{\partial \alpha}\frac{\partial \alpha}{\partial p_1} = \frac{\partial Z}{\partial \alpha}\,,$$
$$\frac{\partial Z}{\partial p_2} = \frac{\partial Z}{\partial \alpha}\frac{\partial \alpha}{\partial p_2}\,,\qquad \frac{\partial Z}{\partial p_3} = \frac{\partial Z}{\partial \beta}\frac{\partial \beta}{\partial \alpha'}\frac{\partial \alpha'}{\partial p_3}\,,$$
$$\frac{\partial Z}{\partial p_4} = \frac{\partial Z}{\partial \alpha}\frac{\partial \alpha}{\partial p_4}\,,\qquad \frac{\partial Z}{\partial p_5} = \frac{\partial Z}{\partial \beta}\frac{\partial \beta}{\partial \alpha'}\frac{\partial \alpha'}{\partial p_5}\,,$$

where

$$\frac{\partial Z}{\partial \alpha} = \frac{\mathrm{i}Z_{\mathrm{f}}}{2p_0}\frac{1}{\sqrt{\alpha\beta}}\Big[\frac{a}{\sin^2(a)} - \cot(a)\Big]\,,\quad a = \frac{\omega\ell}{c_{\mathrm{f}}}\sqrt{\alpha\beta}\,,$$
$$\frac{\partial Z}{\partial \beta} = \frac{\mathrm{i}Z_{\mathrm{f}}}{2p_0}\sqrt{\frac{\alpha}{\beta^3}}\Big[\frac{a}{\sin^2(a)} + \cot(a)\Big]\,,\quad \frac{\partial \beta}{\partial \alpha'} = \frac{\gamma_{\mathrm{f}} - 1}{(\alpha')^2}\,,$$

$$\frac{\partial \alpha}{\partial p_2} = \frac{\omega_*}{\mathrm{i}\omega}\sqrt{\frac{\mathrm{i}\omega}{\omega_*}p_4 + 1}\,,\qquad \frac{\partial \alpha}{\partial p_4} = \frac{p_2}{2\sqrt{\frac{\mathrm{i}\omega}{\omega_*}p_4 + 1}}\,,$$
$$\frac{\partial \alpha'}{\partial p_3} = \frac{\omega'_*}{\mathrm{i}\omega}\sqrt{\frac{\mathrm{i}\omega}{\omega'_*}p_5 + 1}\,,\qquad \frac{\partial \alpha'}{\partial p_5} = \frac{p_3}{2\sqrt{\frac{\mathrm{i}\omega}{\omega'_*}p_5 + 1}}\,.$$

[1] M. E. Delany and E. N. Bazley, "Acoustical properties of fibrous absorbent materials", Appl. Acoust. **3**, 105–116 (1970).

[2] Y. Miki, "Acoustical properties of porous materials – Generalizations of empirical models", J. Acoust. Soc. Jpn. **11**, 19–24 (1990).

[3] Y. Miki, "Acoustical properties of porous materials – Modifications of Delany-Bazley models", J. Acoust. Soc. Jpn. **11**, 25–28 (1990).

[4] K. Attenborough, "Acoustical characteristics of rigid fibrous absorbents and granular materials", J. Acoust. Soc. Am. **73**, 785–799 (1983).

[5] N. Voronina, "Improved empirical model of sound propagation through a fibrous material", Appl. Acoust. **48**, 121–132 (1996).

[6] N. N. Voronina and K. V. Horoshenkov, "A new empirical model for the acoustic properties of loose granular media", Appl. Acoust. **64**, 415–435 (2003).

[7] D. L. Johnson, J. Koplik, and R. Dashen, "Theory of dynamic permeability and tortuosity in fluid-saturated porous media", J. Fluid Mech. **176**, 379–402 (1987).

[8] Y. Champoux and J.-F. Allard, "Dynamic tortuosity and bulk modulus in air-saturated porous media", J. Appl. Phys. **70**, 1975–1979 (1991).

[9] D. Lafarge, P. Lemarinier, J. F. Allard, and V. Tarnow, "Dynamic compressibility of air in porous structures at audible frequencies", J. Acoust. Soc. Am. **102**, 1995–2006 (1997).

[10] S. R. Pride, F. D. Morgan, and A. F. Gangi, "Drag forces of porous-medium acoustics", Phys. Rev. B **47**, 4964–4978 (1993).

[11] O. Umnova and D. Turo, "Time domain formulation of the equivalent fluid model for rigid porous media", J. Acoust. Soc. Am. **125**, 1860–1863 (2009).

[12] J. F. Allard, N. Atalla, *Propagation of Sound in Porous Media: Modelling Sound Absorbing Materials, Second Edition* (Wiley, 2009).

[13] APMR – Acoustical Porous Material Recipes, `http://apmr.matelys.com/` (date last viewed 3/16/2015).

[14] C. Batifol, T. G. Zielinski, M. N. Ichchou, and M.-A. Galland, "A finite-element study of a piezoelectric/poroelastic sound package concept", Smart Mater. Struct. **16**, 168–177 (2007).

[15] T. G. Zieliński, "Fundamentals of multiphysics modelling of piezo-poro-elastic structures", Archives of Mechanics **62**, 343–378 (2010).

[16] T. G. Zieliński, "Numerical investigation of active porous composites with enhanced acoustic absorption", J. Sound Vib. **330**, 5292–5308 (2011).

[17] ISO 9053:1991: "Acoustics – materials for acoustical applications – determination of airflow resistance" (1993).

[18] P. Leclaire, L. Kelders, W. Lauriks, M. Melon, N. Brown, and B. Castagnède, "Determination of the viscous and thermal characteristic lengths of plastic foams by ultrasonic measurements in helium and air", J. Appl. Phys. **80**, 2009–2012 (1996).

[19] Z. E. A. Fellah, S. Berger, W. Lauriks, C. Depollier, C. Aristégui, and J.-Y. Chapelon, "Measuring the porosity and the tortuosity of porous materials via reflected waves at oblique incidence", J. Acoust. Soc. Am. **113**, 2424–2433 (2003).

[20] N. Kino, "Ultrasonic measurements of the two characteristic lengths in fibrous materials", Applied Acoustics **68**, 1427–1438 (2007).

[21] C. Braccesi and A. Bracciali, "Least squares estimation of main properties of sound absorbing materials through acoustical measurements", Appl. Acoust. **54**, 59–70 (1998).

[22] C. Zwikker and C. W. Kosten, *Sound Absorbing Materials* (Elsevier, 1949).

[23] J. Alba, R. del Rey, J. Ramis, and J. P. Arenas, "An inverse method to obtain porosity, fibre diameter and density of fibrous sound absorbing materials", Arch. Acoust. **36**, 561–574 (2011).

[24] N. Voronina, "Acoustic properties of fibrous materials", Appl. Acoust. **42**, 165–174 (1994).

[25] Z. E. A. Fellah, F. G. Mitri, M. Fellah, E. Ogam, and C. Depollier, "Ultrasonic characterization of porous absorbing materials: Inverse problem", J. Sound Vib. **302**, 746–759 (2007).

[26] P. Göransson, R. Guastavino, and N.-E. Hörlin, "Measurement and inverse estimation of 3D anisotropic flow resistivity for porous materials", J. Sound Vib. **327**, 354–367 (2009).

[27] C. Van der Kelen and P. Göransson, "Identification of the full anisotropic flow resistivity tensor for multiple glass wool and melamine foam samples", J. Acoust. Soc. Am. **134**, 4659–4669 (2013).

[28] R. Panneton and X. Olny, "Acoustical determination of the parameters governing viscous dissipation in porous media", J. Acoust. Soc. Am. **119**, 2027–2040 (2006).

[29] X. Olny and R. Panneton, "Acoustical determination of the parameters governing thermal dissipation in porous media", J. Acoust. Soc. Am. **123**, 814–824 (2008).

[30] J.-P. Groby, E. Ogam, L. D. Ryck, N. Seba, and W. Lauriks, "Analytical method for the ultrasonic characterization of homogeneous rigid porous materials from transmitted and reflected coefficients", J. Acoust. Soc. Am. **127**, 764–772 (2010).

[31] N. Dauchez and P.-A. Yvars, "Inverse method for porous material characterization using the constraint satisfaction problem approach", in *Proceedings of the Acoustics 2012 Nantes Conference* (2012), pp. 1961-1965.

[32] P. Bonfiglio and F. Pompoli, "Inversion problems for determining physical parameters of porous materials: Overview and comparison between different methods", Acta Acust. united Ac. **99**, 341–351 (2013).

[33] N. Sellen, M.-A. Galland, and O. Hilbrunner, "Identification of the characteristic parameters of porous media using active control", in *Proceedings of the 8th AIAA/CEAS Aeroacoustics Conference* (2002), AIAA Paper 2002-2504, pp. 1–10.

[34] Y. Atalla and R. Panneton, "Inverse acoustical characterization of open cell porous media using impedance tube measurements", Can. Acoust. **33**, 11–24 (2005).

[35] T. G. Zieliński, "Inverse identification and microscopic estimation of parameters for models of sound absorption in porous ceramics", in *Proceedings of International Conference on Noise and Vibration Engineering (ISMA2012) / International Conference on Uncertainty in Structural Dynamics (USD2012)* edited by P. Sas, D. Moens, and S. Jonckheere (2012), pp. 95–108.

[36] T. G. Zieliński, "A methodology for a robust inverse identification of model parameters for porous sound absorbing materials", in *Proceedings of ISMA2014 – International Conference on Noise and Vibration Engineering* (2014).

[37] A. Wirgin, "The inverse crime" (2004), `arXiv:math-ph/0401050v1` (date last viewed 3/16/2015).

[38] ISO 10534-2: "Determination of sound absorption coefficient and impedance in impedance tubes" (1998).

[39] J. S. Bolton, T. Yoo, and O. Olivieri, "Measurement of normal incidence transmission loss and other acoustical properties of materials placed in a standing wave tube", Technical Review 1, Brüel & Kjaer (2007).

[40] B. H. Song and J. S. Bolton, "A transfer-matrix approach for estimating the characteristic impedance and wave numbers of limp and rigid porous materials", J. Acoust. Soc. Am. **107**, 1131–1152 (2000).

[41] P. C. Hansen, *Mathematical Modeling and Computation Rank-Deficient and Discrete Ill-Posed Problems: Numerical Aspects of Linear Inversion*, (SIAM, 1998), 247 pages.

[42] M. Ouisse, M. Ichchou, S. Chedly, and M. Collet, "On the sensitivity analysis of porous material models", J. Sound Vib. **331**, 5292–5308 (2012).

[43] W. C. Thacker, "The role of the hessian matrix in fitting models to measurements", J. Geophys. Res. **94**, 6177–6196 (1989).

[44] M. Potoczek, "Gelcasting of alumina foams using agarose solutions", Ceram. Int. **34**, 661–667 (2008).

[45] T. G. Zieliński, M. Potoczek, R. E. Śliwa, and Ł. J. Nowak, "Acoustic absorption of a new class of alumina foams with various high-porosity levels", Arch. Acoust. **38**, 495–502 (2013).

[46] T. G. Zieliński, "Generation of random microstructures and prediction of sound velocity and absorption for open foams with spherical pores", J. Acoust. Soc. Am. **137**, 1790–1801 (2015).

[47] J.-P. Dalmont, "Acoustic impedance measurement, Part I: A review", J. Sound Vib. **243**, 427–439 (2001).

[48] J.-P. Dalmont, "Acoustic impedance measurement, Part II: A new calibration method", J. Sound Vib. **243**, 441–459 (2001).

[49] J.-F. Despois and A. Mortensen, "Permeability of open-pore microcellular materials", Acta Materialia **53**, 1381–1388 (2005).

[50] N. J. Mills, *Polymer Foams Handbook: Engineering and Biomechanics Applications and Design Guide*, (Butterworth-Heinemann, 2007), 535 pages.